Silicon (2022) 14:11163–11170
https://doi.org/10.1007/s12633-022-01852-y

ORIGINAL PAPER

Synthesis, Characterization, Morphological, Linear and Nonlinear Optical Properties of Silicon Carbide Doped PVA Nanocomposites

J. Prakash [1] · S. Jeyaram [2]

Received: 28 January 2022 / Accepted: 25 March 2022 / Published online: 5 April 2022

Abstract

This work reports the synthesis, characterization, morphological, linear and nonlinear optical (NLO) features of undoped and silicon carbide (SiC) doped polyvinyl alcohol (PVA) nanocomposites thin films with different doping concentration of SiC. The sample was characterized by UV-Visible, Emission and FT-IR spectrometer, respectively. The morphology of undoped and SiC doped PVA nanocomposites was studied by Field emission scanning electron microscopy (FESEM) and the chemical composition was identified by Energy dispersive X-ray (EDAX) spectra. The FESEM reveals that the SiC nanoparticles are uniformly embedded on PVA and exhibits a spherical shaped structure. The NLO features of the nanocomposite films have been studied by a continuous wave diode laser working at 650 nm wavelength. The closed aperture Z-scan technique divulge the characters of self-defocusing and open aperture Z − scan methods reveals the characteristic property of both saturable absorption (SA) and reverse saturable absorption (RSA). A switch over from SA to RSA was observed in the nanocomposite films by increasing the weight% of SiC. The nonlinear refraction and nonlinear coefficient of absorption of the films was found to be the order of 10^{-12} m^2/W and 10^{-5} m/W, respectively. The experimental results are divulged that the SiC doped PVA nanocomposite films are potential material for optoelectronics applications.

Keywords SiC-PVA nanocomposites · Z − scan · Nonlinear index of refraction · Nonlinear coefficient of absorption

1 Introduction

In the modern technological world, lasers are widely used in different fields such as electronics, industry, medicine, and military [1]. With the rapid increase in the use of laser in numerous applications, there is a necessity to design and develop the nonlinear optical (NLO) materials for photonic and optoelectronics applications [2, 3]. NLO materials are widely used in different area of science and technology such as optical switching, optical limiting for eye and sensor production, optical computing, optical telecommunication, and optical data storage [4–6]. Great efforts have been made to design and develop the different and novel NLO materials such as organic [7–9], inorganic [10, 11], carbon nanotubes [12, 13], nanomaterials [14], natural pigments [15–17] and graphene oxide [18]. Among these materials, nanoparticles have gained significant attention for their excellent optical properties [19–21]. In the last two decades, many different studies have been performed on the nanoparticles, because of their potential applications in the field of photonics due to good thermal and chemical stability with high mechanical strength [22]. Nanoparticles are available in different sizes and shapes. Silicon carbide (SiC) nanoparticles is one among them have received a significant attention due to high conductivity, stability, purity and large thermal expansion coefficient [23, 24].

Composites of polymers and nanoparticles have also received more attention because they open a new pathway for developing novel engineering materials with good electrical, optical, mechanical and magnetic properties [25–27]. PVA is a multi-hydroxyl (O-H) polymer and has been widely applied for electrical and mechanical field due to their high tensile strength, elasticity and degradability [28]. PVA is water soluble polymer, non-toxic with good hydrophilicity and a strong

✉ J. Prakash
prakashphdjuly2014@gmail.com

S. Jeyaram
jeyaram.msc@gmail.com

[1] Department of Mechanical Engineering, School of Engineering and Technology, Surya Group of Institutions, Villupuram 605652, Tamilnadu, India

[2] Department of Physics, School of Engineering and Technology, Surya Group of Institutions, Villupuram 605652, Tamilnadu, India

chemical and mechanical resistance. PVA is widely used in artificial organs, fibers, contact lenses, drug delivery systems, etc. [29]. The nanoparticles-doped polymer composites have also paved the way for new biological investigations [30]. This paper reports the synthesis, characterization, morphological, linear and nonlinear optical (NLO) features of undoped and SiC doped PVA nanocomposites with different weight percentages of SiC nanoparticles for the first time to the best of our knowledge. The NLO behavior of the nanocomposite films was studied by low power continuous wave diode laser working at 650 nm wavelength.

2 Experimental

2.1 Materials

Polyvinyl Alcohol (Mw = 130,000 g/mol) was received from Sigma-Aldrich and used as such. High purity (99.9%) of SiC nanoparticles was purchased from Nanoshel India, India. The average particle size of the SiC nanoparticle is about 45–65 nm. The FESEM image and EDAX spectra of the SiC nanoparticles were reported in our previous work [23]. The presence of SiC nanoparticles is confirmed by the EDAX spectra, which shows a strong signal in the Si region [23].

2.2 Preparation of SiC/PVA Nanocomposite Films

1 g of PVA was dissolved in 100 ml of water, stirred at 80 ^{o}C for 1 h. The known quantity of SiC nanoparticles was added to the polymer solution which is considered as 1 wt%. The SiC doped polymer solution was again stirred using magnetic stirrer at room temperature for 1 h. Similarly, 2 wt% and 3 wt% of SiC nanoparticles was added to polymer solution and stirred for 1 h to get a homogeneous solution. The SiC doped PVA films have been prepared via film casting method and the prepared films were dried at room temperature for 24 h.

2.3 Characterization Methods

The UV-visible absorption spectra of undoped and SiC doped PVA nanocomposite films were recorded using Perkin Elmer Lambda 35. The fluorescence spectra of the films were recoded using Perkin Elmer LS 45 over a range of 200–400 nm. The Fourier transform infrared (FT-IR) spectra of the sample were analyzed by Perkin Elmer Fourier transform infrared spectrophotometer over the range of 400–4000 cm^{-1} with a resolution of 4 cm^{-1}. The morphology of the films was recorded by Carl Zeiss Sigma FE-SEM with acceleration voltage of 20 KV. Nonlinear absorption (β) and nonlinear refraction (n_2) of the prepared nanocomposite films was studied by Z–scan experimental setup as shown in Fig. 1. A CW diode laser source working at 650 nm wavelength with power of 5 mW has been used for performing the Z–scan measurements. The n_2 and β of the nanocomposite films with varying the weight% of SiC were measured by closed and open aperture Z–scan method. In closed aperture configuration, the aperture is placed before the detector in which the central portion of the transmitted beam alone enters into the detector. For open aperture study, the aperture was removed and placed a convex lens before the detector to collect entire transmittance of the beam. A convex lens with focal length of 5 cm was used to focus the beam. The transmittance of the beam at far-field position was measured by a photo detector connected to the digital power meter.

3 Results and Discussion

3.1 UV-Vis Study

Figure 2 depicts the transmittance curve of undoped and SiC doped PVA nanocomposite films over a range of 300–1100 nm. It is observed from Fig. 2 that, the prepared films

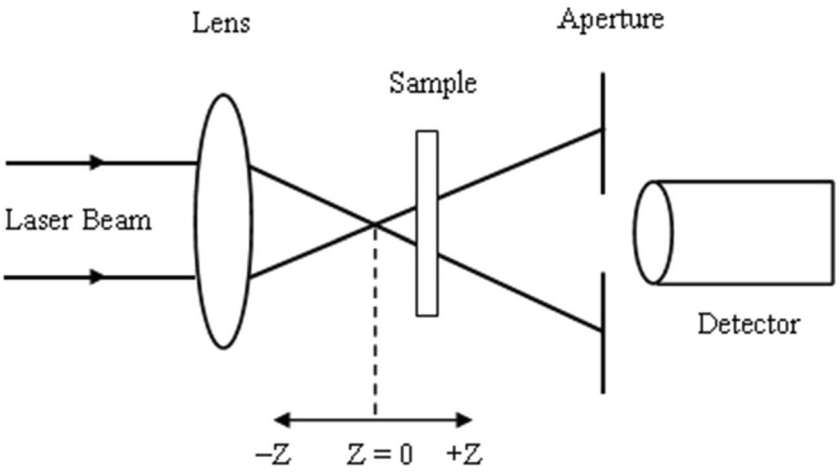

Fig. 1 Experimental Z − scan technique

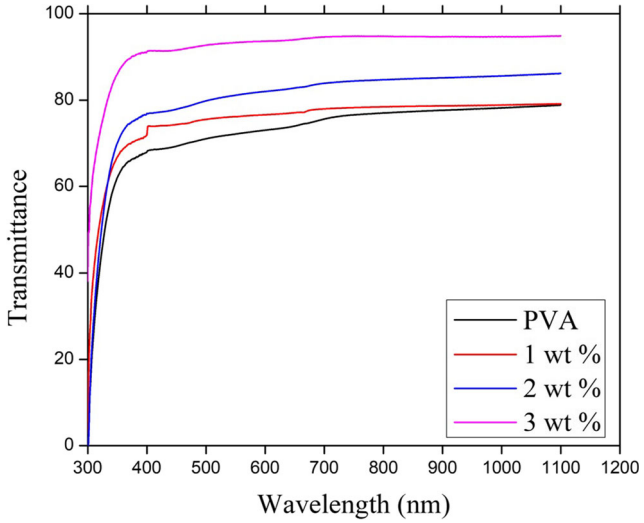

Fig. 2 Transmittance spectra of SiC doped PVA film with different concentration

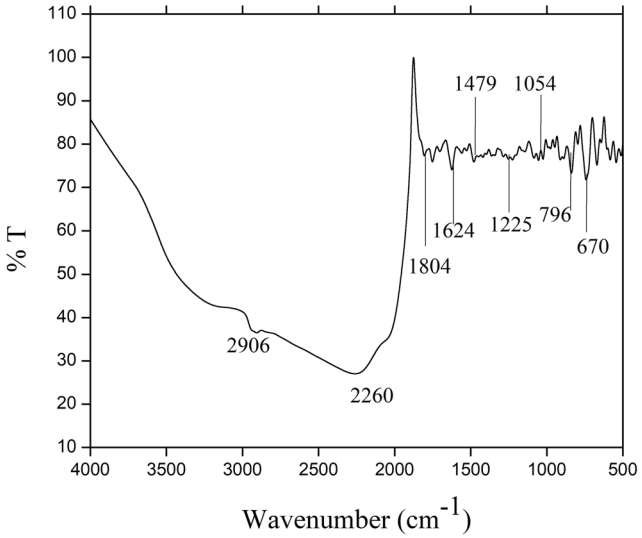

Fig. 4 FT-IR spectra of SiC doped PVA film at 3 wt% concentration

have highly transparent from 400 to 1100 nm and the pure PVA film exhibit higher transmittance of about 94.7%. The transmittance was decreased by increasing the weight% of SiC nanoparticles. When the concentration increases, more absorption take place which result in decrease in transmittance. The transmittance of the films was decreased from 84.8 to 78.5% by increasing the SiC concentration from 1 wt% to 3 wt%. Furthermore, the transmittance of 1 wt%, 2 wt% and 3 wt% of SiC doped PVA nanocomposites are found to exhibit an abrupt decrease in the UV region is the result of strong electron presence within the band gap [31]. This spectral region was considered as significant increase in absorption.

3.2 Emission Study

The emission spectrum of pure PVA and SiC doped PVA nanocomposite films is shown in Fig. 3 with an excitation wavelength of 320 nm. From Fig. 3, the intensity of emission spectra is moderately depends on the nanoparticles concentration. The emission peak intensity of pure PVA, 1 wt%, 2 wt% and 3 wt% of SiC doped PVA was increased by increasing the weight% of SiC nanoparticles. Furthermore, the observation of red shift with enhanced intensity of nanocomposite films is due to increasing the weight% of SiC.

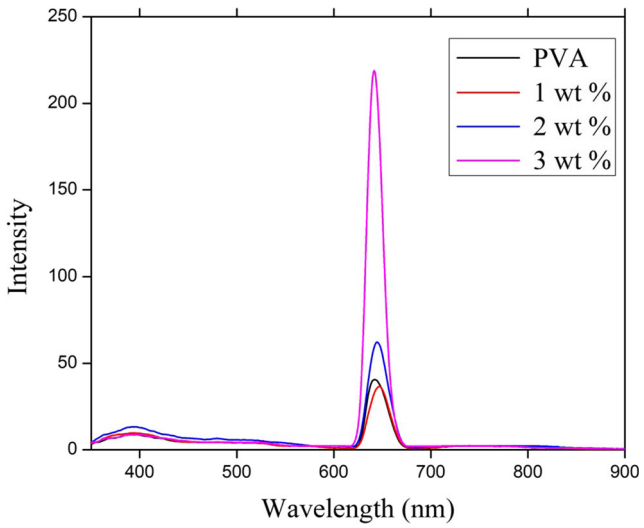

Fig. 3 Emission spectra of SiC doped PVA film with different concentration

Table 1 FT-IR assignments of SiC doped PVA nanocomposite films

Wavenumber (cm^{-1})	Vibrational assignments	Group
670	C=S stretching	Sulfide
796	C=C bending	Alkene
975	C=C bending	Alkene
1054	C−N stretching	Amine
1226	O−H stretching	Alcohol
1479	C=C stretching	Aromatic
1526	C=C stretching	Aromatic
1624	C=C stretching	Alkene
1703	C−H bending	Aromatic compound
1751	C=O stretching	Anhydride
1803	C=O stretching	Conjugated acid halide
2909	O−H stretching	Alcohol
3180	O−H stretching	Alcohol

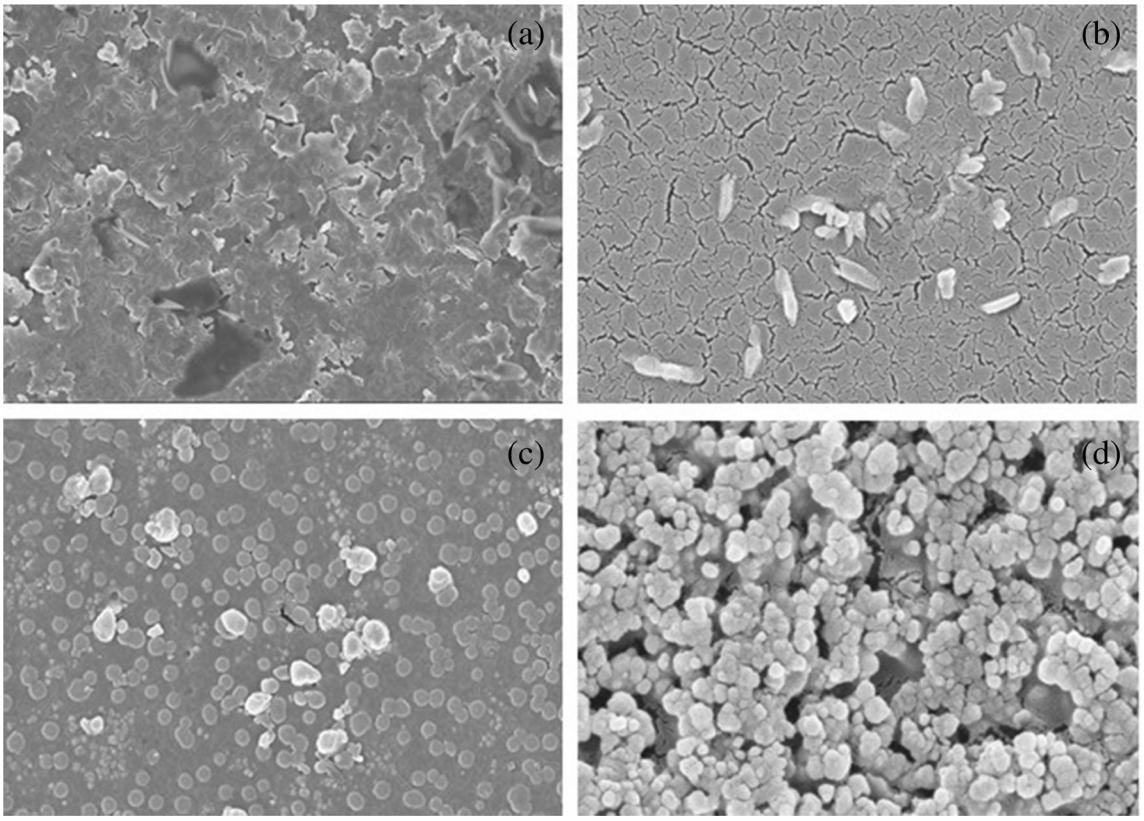

Fig. 5 FESEM image of SiC doped PVA film (**a**) Pure PVA (**b**) 1 wt% SiC doped PVA (**c**) 2 wt% SiC doped PVA (**d**) 3 wt% SiC doped PVA

3.3 FT-IR Study

The FT-IR spectra of 4 wt% of SiC doped PVA nanocomposite film is depicted in Fig. 4 and the corresponding vibrational frequencies is tabulated in Table 1. A strong peak was observed respectively at 3180 cm^{-1} and 2909 cm^{-1} are owing to OH stretching. The frequency band at 1803 cm^{-1} and 1751 cm^{-1} are owing to stretching of C = O groups. The existence of a weak band at 1703 cm^{-1} in the spectra is due to bending of C-H group. The presence of stretching of C = C group is confirmed by the weak bands at 1624 cm^{-1}, 1526 cm^{-1} and 1479 cm^{-1}. A band at 1226 cm^{-1} is consigned to stretching of OH groups. The stretching of groups associated with the frequency range of 1054 cm^{-1}.

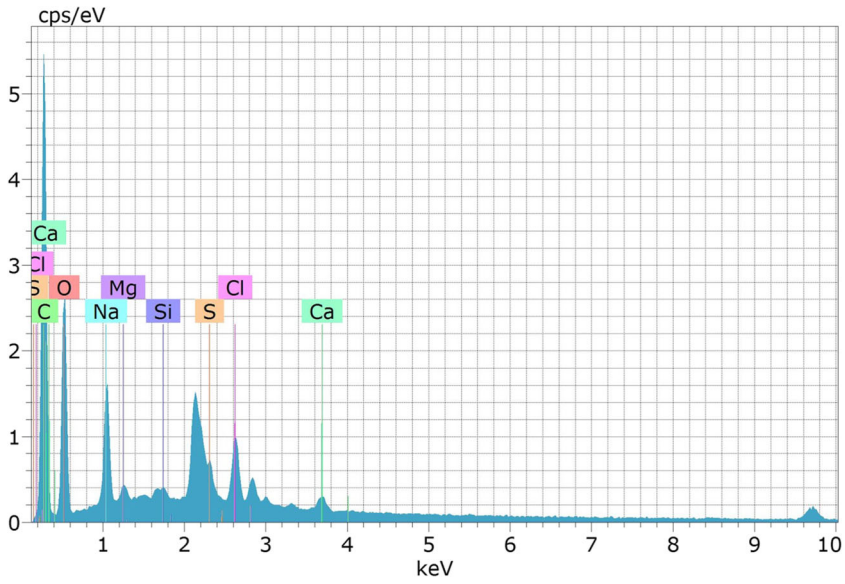

Fig. 6 Energy dispersive X-ray (EDAX) spectra of 3 wt % of SiC doped PVA film

Table 2 Elemental concentration present in SiC doped PVA nanocomposites

Element	Series	Concentration (Wt %)
Carbon	K-series	55.81
Oxygen	K-series	36.31
Sodium	K-series	4.60
Magnesium	K-series	0.23
Sulfur	K-series	0.90
Chlorine	K-series	1.76
Calcium	K-series	0.35
Silicon	K-series	0.01

Furthermore, the frequencies observed at 975 cm^{-1} and 796 cm^{-1} are represents respectively the bending of C = C groups. The weak band observed at 670 cm^{-1} is confirming the presence of sulfide groups in the sample.

3.4 Surface Morphology

The surface morphology of pure PVA and SiC doped PVA nanocomposite films with different weight% of SiC nanoparticles is shown in Fig. 5(a-d). Figure 5(a-d) reveals that the pure PVA film exhibits a smooth surface whereas SiC/PVA nanocomposite films revealed that the inclusion of SiC on the surface of PVA. The well size and spherical shaped particle distribution of SiC through the PVA blend was observed at higher concentration of SiC nanoparticles as shown in Fig. 5(d). Furthermore, the FESEM image of SiC/PVA nanocomposite films confirmed that more aggregation of SiC nanoparticles was existed at a higher concentration of SiC. The chemical composition of the SiC doped PVA nanocomposite films were analyzed by energy dispersive X-ray analysis (EDAX) as shown in Fig. 6. The elemental concentration obtained from EDAX is presented in Table 2.

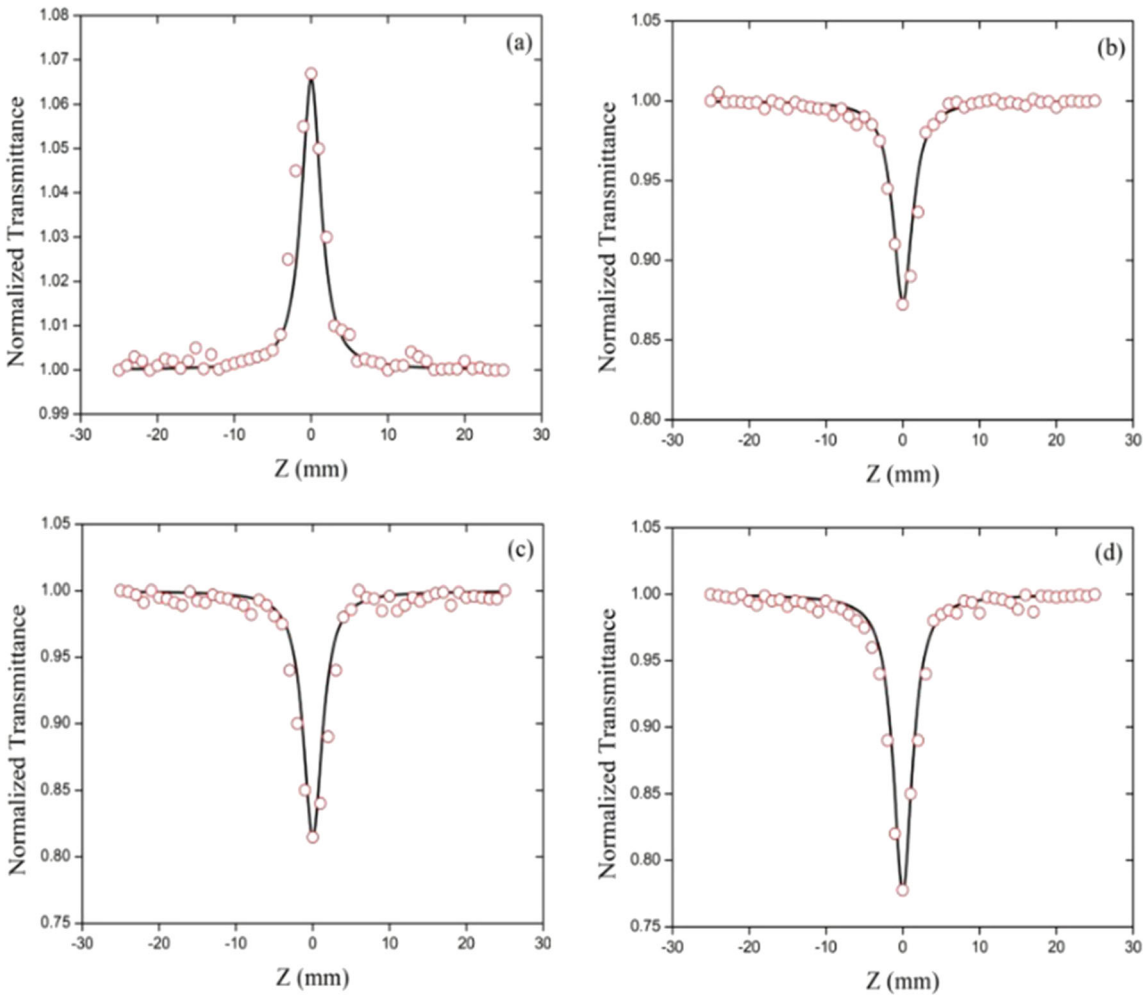

Fig. 7 Open aperture result of SiC doped PVA film (**a**) Pure PVA (**b**) 1 wt% SiC doped PVA (**c**) 2 wt% SiC doped PVA (**d**) 3 wt% SiC doped PVA

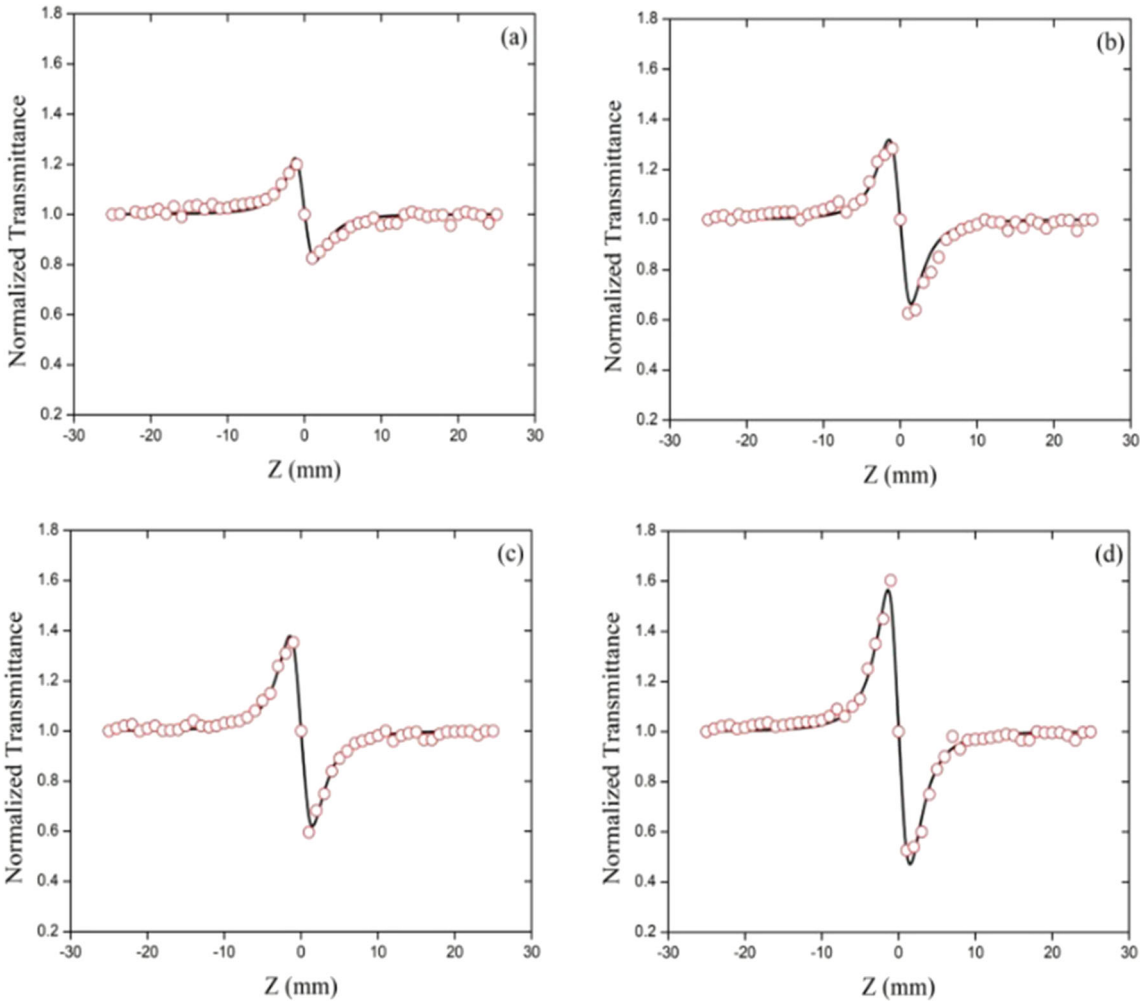

Fig. 8 Pure nonlinear refraction curve of SiC doped PVA film (**a**) Pure PVA (**b**) 1 wt% SiC doped PVA (**c**) 2 wt% SiC doped PVA (**d**) 3 wt% SiC doped PVA

3.5 NLO Study

Third-order NLO features of undoped and SiC doped PVA nanocomposite films have been measured from closed and open aperture Z–scan technique [32]. The closed aperture technique gives the information about nonlinear index of refraction (n_2), while the open aperture method gives the information of nonlinear coefficient of absorption (β). The n_2 and β of the sample is directly related to real and imaginary components of the third-order NLO susceptibility. Figure 7 (a-d) depicts the open aperture Z–scan traces of undoped and SiC doped PVA nanocomposite films with different weight percentages. The nonlinear absorption coefficient (β) of the films displays both SA and RSA or two-photon absorption (TPA) behaviors. It is observed from Fig. 7 (a) that, the pure PVA film exhibits the characteristic features of saturable absorption. The increase in transmission with respect to the intensity of incident radiation at the focus is the result of SA. Alternatively, SiC doped PVA films with different weight percentages of SiC nanoparticles exhibits positive nonlinear

Table 3 Measured third-order NLO properties of SiC doped PVA nanocomposites

Sample	$n_2 \times 10^{-12}$ (m^2/W)	β X 10^{-5} (m/W)	Re (χ^3) X 10^{-7} (esu)	Im (χ^3) X 10^{-7} (esu)	$\chi^{(3)}$ X 10^{-7} (esu)
Pure PVA	– 1.99	– 0.35	– 0.64	– 0.06	0.64
1 wt%	– 3.49	0.66	– 1.13	0.11	1.14
2 wt%	– 4.03	0.96	– 1.30	0.16	1.31
3 wt%	– 5.64	1.14	– 1.82	0.19	1.83

coefficient of absorption is the consequence of RSA as shown in Fig. 7 (b-d). A switchover from SA to RSA occurs in the composite films as the result of increasing the concentration of SiC nanoparticles. It is also observed from Fig. 7 (b-d) that the increased valley depth with increase in SiC nanoparticle concentration is ascribed to increase in two-photon absorption coefficient (β). The β of the composite films is obtained from the fitting curve of open aperture data to the following equation [31]:

$$T(z, S=1) = \frac{C(1+z^2/z_0^2)}{\sqrt{\pi}\beta I_0 L_{eff}} \int_{-\infty}^{+\infty} In\left(1+\frac{\beta I_0 L_{eff} e^{-t^2}}{(1+z^2/z_0^2)}\right) dt \quad (1)$$

where C is the constant, I_o is the input irradiance at the focus and L_{eff} is the effective thickness of the sample. The measured nonlinear coefficient of absorption β of the nanocomposite films are presented in Table 2. From Table 2, the higher value of β is obtained at 3 wt% of SiC doped PVA nanocomposite film.

The n_2 of undoped and SiC doped PVA nanocomposite film is determined from closed aperture Z–scan method. Figure 8 (a-d) shows the pure nonlinear refraction curve of undoped and SiC doped PVA nanocomposite films. The pure nonlinear refraction is obtained by diving closed aperture data by corresponding open aperture data. The refraction curve exhibits a pre focal transmittance followed by post focal transmittance minimum is the characteristic features of negative nonlinear index of refraction i.e., self-defocusing. The self-defocusing effect in the films is the consequence of thermal nonlinearity which arises from absorption of laser irradiation at 650 nm wavelength. Furthermore, the peal-valley difference increases with increase in SiC concentration. The transmittance of the nanocomposite films is determined from the fitting curve of closed aperture using the relation,

$$T(z) = 1 - \Delta\emptyset_0 \frac{4X}{(X^2+1)(X^2+9)} \quad (2)$$

where $X = Z/Z_0$. The n_2 of the nanocomposite film is given by

$$n_2 = \frac{\Delta\emptyset_o \lambda}{2\pi I_0 L_{eff}} \left(\frac{cm^2}{W}\right) \quad (3)$$

where $\Delta\emptyset_0$ and λ are the on-axis phase shift and laser beam wavelength. The real and imaginary components of the third-order optical nonlinearity is given by,

$$Re\left[\chi^{(3)}\right](esu) = 10^{-4} \frac{\varepsilon_0 c^2 n_0^2}{\pi} n_2 \left(\frac{cm^2}{W}\right) \quad (4)$$

$$Im\left[\chi^{(3)}\right](esu) = 10^{-2} \frac{\varepsilon_0 c^2 n_0^2 \lambda}{4\pi^2} \beta \left(\frac{cm}{W}\right) \quad (5)$$

where ε_0 and c are the permittivity of free space and light velocity in vacuum. Third-order NLO susceptibility $\chi^{(3)}$ of the nanocomposite film is calculated by,

$$\chi^{(3)} = \sqrt{(Re(\chi)^{(3)})^2 + (Im(\chi)^{(3)})^2}(esu) \quad (6)$$

The third-order NLO parameters of undoped and SiC doped PVA nanocomposite films are presented in Table 3. It is observed from Table 2 that, the nonlinear optical susceptibility of the prepared nanocomposite films exhibit a large optical nonlinearity at higher concentration of SiC nanoparticles. .

4 Conclusions

The undoped and SiC doped PVA nanocomposites with different weight percentages of SiC was prepared by simple casting method. The functional group present in the nanocomposite film was examined by Fourier transform infrared spectroscopy. Morphology of pure PVA and different weight percentages of SiC doped PVA was studied by FESEM and it reveals that the SiC nanoparticles was uniformly embedded on PVA. The NLO features of the nanocomposite films were studied by using Z–scan technique with low power CW laser. The nonlinear refraction and nonlinear absorption of the films were studied from closed and open aperture technique, respectively. The real and imaginary features of undoped and SiC doped PVA nanocomposite films were found to be the order of 10^{-7} esu. A remarkable NLO susceptibility was observed at higher concentration of SiC nanoparticles. The experimental results divulge that the prepared nanocomposite film is a potential material for future photonics and optoelectronics applications.

Author Contribution All authors have equally contributed.

Data Availability All the data available with the authors.

Declarations

Ethics Approval The submitted work should be original and should not have been published elsewhere in any form or language.

Consent to Participate Yes.

Consent for Publication Yes granted.

Competing Interests The authors have declared that no competing interests exist.

Conflict of Interest The authors declare that they have no conflict of interest.

Research involving Human Participants and/or Animals Research involving human participants.

Informed Consent Not applicable.

References

1. Herriott DR (1968) Applications of laser light. Natl Acad Sci Eng Med 219:140–156
2. He GS, Zhao CF, Bhawalkar JD, Prasad PN (1995) Two photon pumped cavity lasing in novel dye doped bulk matrix rod. Appl Phys Lett 67:3703
3. Bass JM, Enoch M, Stryland EV, Wolfe WL (2001) Handbook of optics IV, fiber optics and nonlinear optics. McGraw-Hill, New York
4. Jamshidi-Ghaleh K, Salmani S, Majles Ara MH (2007) Nonlinear response and optical limiting behavior of fast green FCF dye under a low power CW He-Ne laser irradiation. Opt Commun 271:551–554
5. Jeyaram S, Geethakrishnan T (2017) Low power laser induced NLO properties and optical limiting of an anthraquinone dye using Zscan technique. J Mater Sci Mater Elect 28:9820–9827
6. Hernandez FZ, Marcano AO, Alvarado Y, Biondi A, Maillotte H (1998) Measurement of nonlinear refraction index and two-photon absorption in a novel organometallic compound. Opt Commun 152:77–82
7. Meng Q, Yan W, Yu M, Huang (2003) A study of third-order nonlinear optical properties for anthraquinone derivaties. Dyes Pigm 56:145–149
8. Jeyaram S, Geethakrishnan (2017) Third-order nonlinear optical properties of acid green 25 dye by Zscan technique. Opt Laser Technol 89:179–185
9. Motiei H, Jafari A, Naderali R (2017) Third-order nonlinear optical properties of organic azo dyes by using strength of nonlinearity parameter and Zscan technique. Opt Laser Technol 88:68–74
10. McEwan K, Lewis K, Yang GY, Chng LL, Lee YW, Lau WP (2003) Synthesis, Characterization, and nonlinear optical study of metalloporphyrins. Adv Funct Mater 13:863–867
11. Ramki C, Ezhil Vizhi R (2018) Insight on the growth and property studies of inorganic hydrated borate (Na_6 $[B_4O_5$ $(OH)_4]_3$. $8H_2O$) single crystal- An effective third order nonlinear optical (NLO) material for optical limiting application. Mater Chem Phys 205: 138–146
12. Zeng H, Han J, Qian D, Gu Y (2014) Third-order nonlinear optical properties of multiwalled carbon nanotubes modified by CdS nanoparticles. Optik 125:6558–6561
13. Yamashita S (2019) Nonlinear optics in carbon nanotube, graphene, and related 2D materials. APL Photonics 4:034301
14. Shokoufi N, Nouri Hajibaba S (2019) The third-order nonlinear optical properties of gold nanoparticles-methylene blue conjugation. Opt Laser Technol 112:198–206
15. Jeyaram S (2021) Spectral, third-order nonlinear optical and optical switching behavior of β-carotenoid extracted from phyllanthus niruri. Indian J Phys. https://doi.org/10.1007/s12648-021-02122-0
16. Jeyaram S, Geethakrishnan T (2020) Spectral and third-order nonlinear optical characteristics of natural pigment extracted from coriandrum sativum. Opt Mater 107:110148
17. Zongo S, Sanusi K, Britton J, Mthunzi P, Nyokong T, Maaza M, Sahraoui B (2015) Nonlinear optical properties of natural laccaic acid dye studied using Z–scan technique. Opt Mater 46:270–275
18. Liu Z, Zhang X, Yan X, Chen YS, Tian JG (2012) Nonlinear optical properties of graphene-based materials. Chin Sci Bull 57: 2971–2982
19. Mousavi M, Nadafan M, Tabatabai Yazdi Sh (2021) Third-order optical nonlinear properties of Co-doped V_2O_5 nanoparticles. Optik 226:165925
20. Nagarajan C, Annie Sujatha R, Mani Rahulan N, Angeline L, Flower V (2020) Optical nonlinearities of centrosymmetric pre and cerium doped tungstate dumbbell shaped nanoparticles. Opt Mater 110:110512
21. Azlina Y, Azlan MN, Halimah MK, Umar SA, El-Mallawany R, Najmi G (2020) Optical performance of neodymium nanoparticles doped tellurite glasses. Phys B Condens Matter 577:411784
22. Ando M, Kadoo K, Haruta M, Sakaguchi T, Miya M (1995) Large third-order optical nonlinearities in transition metal oxides. Nature 374:625–627
23. Prakash J, Gopalakrishnan S, Kalyana Chakaravarthy V (2021) Mechanical characterization studies of Aluminium Alloy 7075 based nanocomposites. Silicon. https://doi.org/10.1007/s12633-021-00979-8
24. Prakash J, Gopalakrishnan S (2021) Teaching-Learning based optimization coupled with response surface methodology for micro chemical machining of aluminium nanocomposite. Silicon 13:409–432
25. Zhu X, Wang J, Nguyen D, Thomas J, Norwood RA, Peyghambarian N (2012) Linear and nonlinear optical properties of Co3O4 polyvinyl-alcohol thin films. Opt Mater Express 2:103–110
26. Turaka S, Vijaya Kumar Reddy K, Sahu RK, Katiyar JK (2021) Mechanical properties of MWCNTs and graphene nano particles modified glass fibre-reinforced polymer nanocomposites. Bull Mater Sci 44:194
27. Patel VK, Chauhan S, Katiyar JK (2018) Physico-mechanical and wear properties of novel sustainable sour-weed fiber reinforced polyester composites. Mater Res Express. https://doi.org/10.1088/2053-1591/aabdd4
28. Menazea AA, Ismail AM, Awwool NS, Ibrahium HA (2020) Physical characterization and antibacterial activity of PVA/Chitosan matrix doped by selenium nanoparticles prepared via one-pot laser ablation route. J Mater Res Tech 9:9598–9606
29. Singh P, Gupta PN, Saroj AL (2020) Ion dynamics and dielectric relaxation behavior of PVA-PVP-NaI-SiO2 based nanocomposites polymer blend electrolytes. Phys B Condens Matter 578:411850
30. Rangappa SM, Siengchin S, Dhakal HN (2020) Green-composites: ecofriendly and sustainability. Appl Sci Engg Prog. https://doi.org/10.14416/j.asep.2020.06.001
31. Alsaad AM, Ahmad AA, Dairy ARaoufA, Ayah S, Al-anbar QM, Al-Bataineh (2020) Spectroscopic characterization of optical and thermal properties of (PMMA-PVA) hybrid thin films doped with SiO_2 nanoparticles. Results Phys 19:103463
32. Jeyaram S (2021) Study of third-order nonlinear optical properties of basic violet 3 dye in polar protic and aprotic solvents. J Fluores 31:1637–1644